Journal of Applied Geophysics 189 (2021) 104326

Contents lists available at ScienceDirect

Journal of Applied Geophysics

journal homepage: www.elsevier.com/locate/jappgeo

Geophysical survey of Tunnug mound periphery, Tuva, Russia

Dmitry Edemsky, Alexei Popov, Igor Prokopovich *

Pushkov Institute of Terrestrial Magnetism, Ionosphere and Radio Wave Propagation, RAS (IZMIRAN), Moscow, Troitsk, Russia

ARTICLE INFO

Article history:
Received 20 February 2020
Received in revised form 5 April 2021
Accepted 8 April 2021
Available online 14 April 2021

Keywords:
Archaeological geophysics
Magnetic survey
GPR
Tunnug
Scythian Burial Mound
Republic of Tuva
Russia

ABSTRACT

The article presents the results of applying integrated geophysical approaches, in particular, magnetometry and ground penetrating radar (GPR) to study complex ritual and funeral architecture of early Scythian mound Tunnug 1 located in the Uyuk river valley, the Republic of Tuva. The total area of the geophysical survey was more than 12,000 m^2. The results of the survey show that the simultaneous use of two geophysical methods, based on different physical principles, gives a full view of the structure of such a complex burial as an early Scythian mound periphery. GPR and magnetometric measurements complement each other and increase the reliability of a detailed geophysical study of complicated archaeological features in difficult, poorly drained, swampy areas and in the presence of permafrost with a nonuniform depth of thawing. GPR adequately displays all the characteristic of subsurface stone structures recorded using magnetometry which is the most popular method of geophysical survey of mounds. It is shown that the use of GPR for this type of archaeological sites is currently underestimated. The results of geophysical work revealed the location of archaeological features at the mound periphery, which will allow a more efficient and justified selection of the excavation sites.

1. Introduction

Tunnug 1 mound (Fig. 1) is located in the central part of the Turano-Uyuk depression (700–1100 m above sea level), the Republic of Tuva, in a low swampy floodplain of the Uyuk river valley. The relief of this area is formed by a mountainous valley with a developed system of floodplains and floodplain terraces, on one of which the mound is located. The ground-soil stratum of the territory has a similar structure and is represented by a modern humus layer, 5 to10 cm thick, and an underlying sub-horizontal structure of interlayers of loam, buried soils and sand. Poor drainage of the territory leads to waterlogging and the appearance of permafrost at the depth of about 1 m. The active manifestation of the permafrost creates significant difficulties during archaeological work, including drainage of the territory, sweeping along the wet layer, cryogenic movement of archaeological material.

The construction of this tomb, similar to the earliest identified Scythian mound Arzhan 1 (Zaitseva et al., 2007), has a regular round shape with a diameter of more than one hundred meters. The height above the present earth surface is a little more than a meter. Under a partially turfed stone platform lies a radial structure of larch logs, in the center of which, presumably, the main burial is located. Ruined log cabins around the center can be spotted from the surface as stone platform drawdowns.

Tunnug 1 belongs to the oldest Scythian cultural horizon of 8-9th century BCE, probably precedes Arzhan 1. This mound is a part of the Valley of Kings archaeological complex, Southern Siberia, which is considered as one of the most important archaeological areas for studying the "Scythian" material culture and the emergence of mobile nomadic cattle breeding. The mound must be considered as a complex archaeological monument consisting of the mound itself and the adjacent structures and territories – mound periphery. The periphery of a large mound may include ditches, ramparts, sacrificial complexes, ritual roads, stone platforms and stone rings encircling the tomb (Parzinger et al., 2016).

For a long time little attention was paid to mound peripheries. However, it is precisely here where traces of funeral feast can be found, represented as bonfires, pavements, places of worship and ritual burial grounds of both people and animals, containing a wide variety of accompanying equipment. All these structures and features are being shreds of evidence of the religious and cult practice of the funeral and memorial cycle of ancient nomads. Their finding and study can make a significant contribution to the understanding of the worldview of the Scythian population. It should be noted that nearby surroundings were continuously used as a place for religious events and ritual burials by the tribes living in this area afterwards.

Geophysical methods are an important part of the scientific toolkit currently used by archaeologists. The basis of these methods is that the physical and chemical properties associated with buried archaeological features are different from ones associated with underground environment (Clark, 1990; Gaffney and Gater, 2003). The first application of geophysical method was apparently noted in 1938 by electrical resistivity survey of a burial complex, Virginia, USA (Bevan, 2000).

* Corresponding author.
E-mail address: prokop@izmiran.ru (I. Prokopovich).

https://doi.org/10.1016/j.jappgeo.2021.104326
0926-9851/

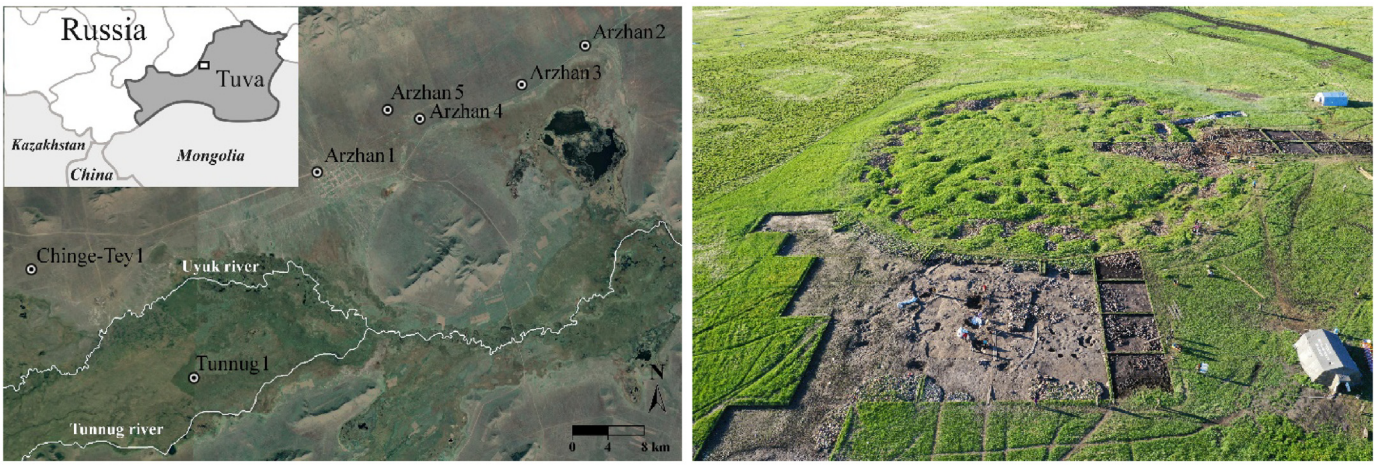

Fig. 1. Map and aerial view of the Tunnug 1 mound.

Recently, more and more archaeological prospections have been carried out using integrating geophysical survey including GPR, magnetic and ERT methods that significantly increases the effectiveness of these search work (Maki and Fields, 2010; Leucci et al., 2015; Di Maio et al., 2016; Welc et al., 2017).

The purpose of this work was to study the mound periphery by geophysical methods: magnetometry and ground penetrating radar (GPR) in order to accurately localize archaeological features and determine the boundaries of the object under study. These geophysical results were taken into account by archaeologists to select excavation sites, determine the scope of work, and plan their implementation.

Such complex archaeological sites as a mound and its periphery can be quite different in composition, structure and, as a result, may have various electrical, magnetic, hydrogeological, and lithological characteristics. Therefore, to obtain the most comprehensive and objective research results, it is reasonable to use an integrated approach where various geophysical methods are applied in order to probe the subsurface environment and to study the archaeological site (Caspari et al., 2019; Welc et al., 2017).

2. Methodology

An efficient way to study the periphery of a burial mound is the use of geophysical methods, such as magnetometry (Parzinger et al., 2016; Fassbinder, 2016), which is based on the identification of anomalies in the earth's magnetic field by measuring magnetic induction vector (module or three vector components). The physical reason for the magnetic field anomalies consists of different magnetic properties of archaeological features in comparison with the surrounding natural environment.

The geoelectric study of soil resistivity is generally accepted as a promising method for the localization of stone structures in the subsurface medium (Schmidt, 2009; Fernandez-Alvarez et al., 2017). However, this method works well only for homogeneous host media without sharp changes in electrical conductivity. The presence of relatively shallow frozen rocks on the entire low floodplain of the Uyuk river valley and their uneven thawing in the spring-summer season, leads to the appearance of significant heterogeneities in the electrical conductivity of the surrounding medium, which can significantly exceed the expected signal levels from artificial stone structures. This, in our opinion, is the main reason for the inefficiency of applying geoelectric resistivity surveys to detect stone structures in the spring-summer period, which was noted in the report (Caspari et al., 2019).

Another perspective geophysical method to be used at archaeological features is the GPR survey. Nowadays ground penetrating radar is a commonly acknowledged and efficient tool of civil engineering and geotechnical inspection of soils at depths from several centimeters to tens of meters (Conyers, 2016; Prokopovich et al., 2018). The principle of operation of GPR is based on the emission of short ultra-wideband electromagnetic pulses into the underlying medium and the registration of reflections from electromagnetic contrast interfaces, layers or features with different conductivities and dielectric constants. The use of geophysical equipment, located on unmanned aerial vehicles drones, looks very promising for future archaeological prospection works (Linck and Kaltak, 2019).

To conduct the present survey around the mound, taking into account the mosaicity of archaeological excavations, the examined territory was divided into fifteen sections with sizes from 8 × 16 to 40 × 48 m so as to cover the entire area of the mound periphery (Figs. 2 and 3a), where places of religious practice of nomads can be found (Caspari et al., 2019). In the southern part of the monument, sites Nos. 1–3 and Nos. 13–15 are adjacent to the main excavation of 2018. The geophysical survey of the periphery of the mound was carried out in the period from May 08 to 25, 2019. The total area of the geophysical survey consists of more than 12,000 square meters.

2.1. Magnetometry

For magnetometric examination in archaeological geophysics, along with most popular fluxgate magnetometers, proton and quantum ones, having higher sensitivity, can be used when measuring the magnitude of the magnetic induction vector (Fassbinder, 2016). Our magnetometric mapping of Tunnug 1 was carried out using a Minimag proton magnetometer applied in exploration geophysics (Ruhunusiri and Jayananda, 2008). This device provides high reliability and stability, its design allows one to work in motion with a distance from the sensor to the earth surface about 0.3–0.4 m.

In order to compensate for the short-term and daily variations of the earth's magnetic field in the measurement results, a base magnetometer was installed in the immediate vicinity of the feature. Methodological support to the work was provided by the IZMIRAN Space Weather Forecast Center (Gaidash et al., 2017), mainly by predicting magnetic activity and preventing the occurrence of magnetic storms during which measurements are impractical.

Geophysical prospecting of Scythian kurgans and their peripheries in the Eurasian Steppe, Siberia, Altai, as well as in the Volga steppe, Caucasus, Kazakhstan and Ukraine have been in focus of geophysical prospecting for more than 20 years. The majority of this work was done by magnetometry. The main reason for this is the fact that the majority of kurgans in the steppe was made of clay, mud, sod, and layers of

tree-bark. In the area of the Valley of the Kings, the first geophysical work using a magnetometer was done in 1998 during the examination of mound Arzhan 2 (Fassbinder and Becker, 2010).

2.2. Ground penetrating radar (GPR)

GPR was introduced into archaeology prospection following a survey conducted in Chaco Canyon, New Mexico in 1974–1976 (Conyers, 2016). Currently, the use of georadars for the detection and mapping of buried archaeological artifacts has already become widespread (Zhao et al., 2015; Bianco et al., 2019; Barone et al., 2020).

In our studies, an enhanced-power GPR of the Loza series was used (Kopeikin et al., 2007). The use of an antenna system with a central frequency of 300 MHz ensured efficient ground probing at depths from tens of centimeters to 2–3 m.

When processing and interpreting the obtained data, the main attention was paid to selecting ground layers, detecting their boundaries, reducing the radargram to the true depth scale and taking into account the velocity of radar signal propagation in the medium. The layers in the GPR depth profile were selected using the procedure of delimiting maxima and minima of the reflected signal, extracting and analyzing the signal in-phase axes, representing the radar cross-section both in "linear" and "derivative" mode of the amplitude function – procedures implemented in the Krot software (Kopeikin et al., 2007).

For the correct interpretation of the obtained radar data and restoration of geological structures, GPR vertical sounding was carried out at selected points of the mound periphery, using the common midpoint (CMP) method (Jol, 2009), which allowed the determination of the electromagnetic wave propagation velocity in the subsurface medium and recalculation of the GPR profile from the time- to the depth scale without attracting a priori information.

It should be noted that a characteristic feature of this expedition was the involvement of two independent teams, with different equipment, experience and methodology, to conduct thorough examination of the complex ritual and funerary architecture of early Scythian mound Tunnug 1. Magnetometric survey had been successfully used earlier to examine other large mounds (Parzinger et al., 2016; Fassbinder, 2016), and geoelectric resistivity measurements were performed by the Swiss team at this object as well – their results are presented in (Caspari et al., 2019). Our data and the results of (Caspari et al., 2019) turned to be close to each other, both reflecting the principal features of the burial complex periphery. They are quite interesting from the methodological point of view, since the work was carried with the equipment of different design, and different approaches were used to process and display the final results.

3. Survey results

3.1. Magnetic survey

The survey sites were marked with clear reference to the topographic map and taking into account the possibility to move along parallel profiles laid in the south-to-north direction. Spatial positioning was carried out manually by an operator with a step of 0.25 or 0.5 m, the larger step 0.5 m was selected only at site No 15 due to a complete absence of significant magnetic anomalies. The length of the profile was determined by the site geometry and varied from 8 to 40 m. The distance between the parallel paths was about 0.5 m.

In order to select regional and local anomalies during data processing, we applied averaging of the magnetic field and compensated daily variations of the Earth's magnetic field by the data of a base magnetometer. The identification of local magnetic anomalies was performed by subtracting slow trends of the regional field. These transformations were performed along each GPR scan. After preliminary data processing, magnetic data taken on different days in the neighboring areas were stitched together at their borders.

After processing the obtained information, a map of the magnetic field of the examined sections was constructed (Fig. 2). The overall magnetic map of the mound is characterized by an uneven set of local anomalies with the significantly irregular magnetic susceptibility of individual stone fragments, as well as complex stone structures forming these archaeological features. The analysis of individual samples shows that a significant part of the stones examined at the excavation site has too low magnetic susceptibility to be registered during magnetic survey, and the amount of interference associated with the presence of black metal in the soil was minimal. These studies were carried out by the authors and previously published (Edemsky et al., 2020). The presentation form of the magnetic map was chosen in shades of gray with a non-linear scale, which allows one to visualize and analyze in more detail weak artificial object signatures on the natural background (60,300 ± 5–15 nT), the diurnal variations of Earth's magnetic field being measured by a static base magnetometer.

On the magnetogram of the spots surrounding the northern and eastern edges of the mound, a discontinuous strip of elongated anomalies reveals an obvious stone ring. This structure is observed from sections No. 3, No. 4 to section No. 10, the ring is located at a distance of 12–16 m from the shaft surrounding the mound. A partial excavation of the stone ring (Sadykov et al., 2020) revealed the structures similar to the stone ritual walls of Arzhan 2 (Čugunov et al., 2010), but of a smaller diameter and located closer to the mound.

In the southern part of the mound, one can distinguish patches No. 1–3 where local stone structures with a diameter of 8–10 m are clearly seen, some of which are partially unsealed by the excavations. Separate stone structures are located quite close to each other, forming a single feature. In the areas from No. 6 to No. 10, no pronounced magnetic anomalies outside the stone ring were recorded. In areas Nos. 13–15, magnetometric studies did not reveal noticeable stone structures.

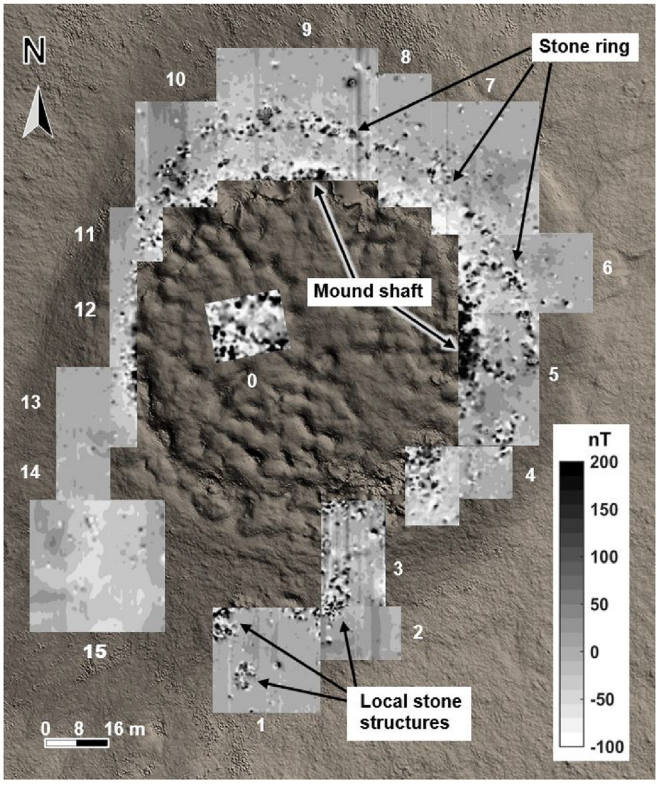

Fig. 2. Magnetic map of the mound periphery. Inserts No 0–15 – geophysical analysis sites with magnetic survey results.

3.2. GPR survey

GPR inspection of the mound periphery was carried out using the method of areal GPR sounding: selected area was crossed with a set of parallel profiles spaced by 0.5 m, with a fixed measurement step of 0.25 m along the profile.

Based on the data obtained, a three-dimensional (3D) model (layered volumetric pattern) of the site has been built. For better analysis, both horizontal XY and vertical cross sections XT, YT can be used, X axis directed from west to east and Y axis – from south to north.

In the points indicated in Fig. 3a by stars, we estimated the electromagnetic wave propagation velocity using the common midpoint (CMP) method (Jol, 2009). In these measurements, the GPR data were recorded with a gradual change in the distance between the transmitting and receiving antennas, from 0.2 m to 4 m with an increment of 0.1 m, which made it possible to draw a hodograph (Fig. 3b) and estimate the electromagnetic wave velocity in the subsurface medium. According to the results of GPR probing by the CMP method, in a thawed, saturated soil the sounding signal propagates about 0.08 m/ns, whereas in drier places the electromagnetic wave velocity reaches 0.13–0.19 m/ns. For further depth estimates, throughout the entire territory of the mound, a characteristic velocity of 0.08 m/ns was assumed.

Based on the results of GPR sounding of individual sites, an integrated 3D GPR model of the burial hill periphery has been constructed. A cross-section of the constructed 3D GPR model of the mound periphery in XY plane at the delay time value of 15 ns (depth about 0.5 m) is shown in Fig. 3a. The amplitude of the signal reflected from local subsurface features, inhomogeneities or interfaces of the soil stratum is represented in a color saturation scale. By analyzing the 3D model and individual linear GPR scans one can localize positions of the anomalies, their geometric dimensions and occurrence depth.

Geophysical analysis of GPR data is more complicated compared to magnetometric ones, because the georadar return signal contains the reflections not only from artificial features embedded into the subsurface medium, but also from all electromagnetic contrasting inhomogeneities caused by the structure changes of the underlying surface, humidity of individual layers, permafrost level, etc.

To the south of the mound, at site No. 1 and at the border of sites No. 2 and No. 3, local anomalies with a diameter of 8–10 m can be distinguished without additional processing. They coincide by location with the features identified in the magnetograms. In the northern and eastern part of the hill periphery, an anomaly is revealed in the form of a strip, up to 8 m wide, located at a distance of 10–12 m from the shaft surrounding the mound. This structure is fixed in sections Nos. 8–13.

Along with specific archaeological data, the GPR sounding results also contain information on the geological structure of the subsurface environment around the monument, allowing one to identify the areas of artificial origin with broken sub-horizontal layering, localize areas of enhanced humidity and thawing zones.

4. Discussion

4.1. Survey environment

For better understanding the results of the complex geophysical survey, it is worth giving a general description of the subsurface medium. According to geophysical data, the examined area presents a soil-ground stratum with a sub-horizontal structure (Fig. 4), consisting of a modern humus horizon, a homogeneous grayish-yellow loamy layer of the parent rock (1), a thin buried meadow-alluvial soil (2), a formation of alternating interlayers of sand and a well-defined layer of ferruginous fine-grained sand (3) at a depth of about 0.8 m. Below, there is a

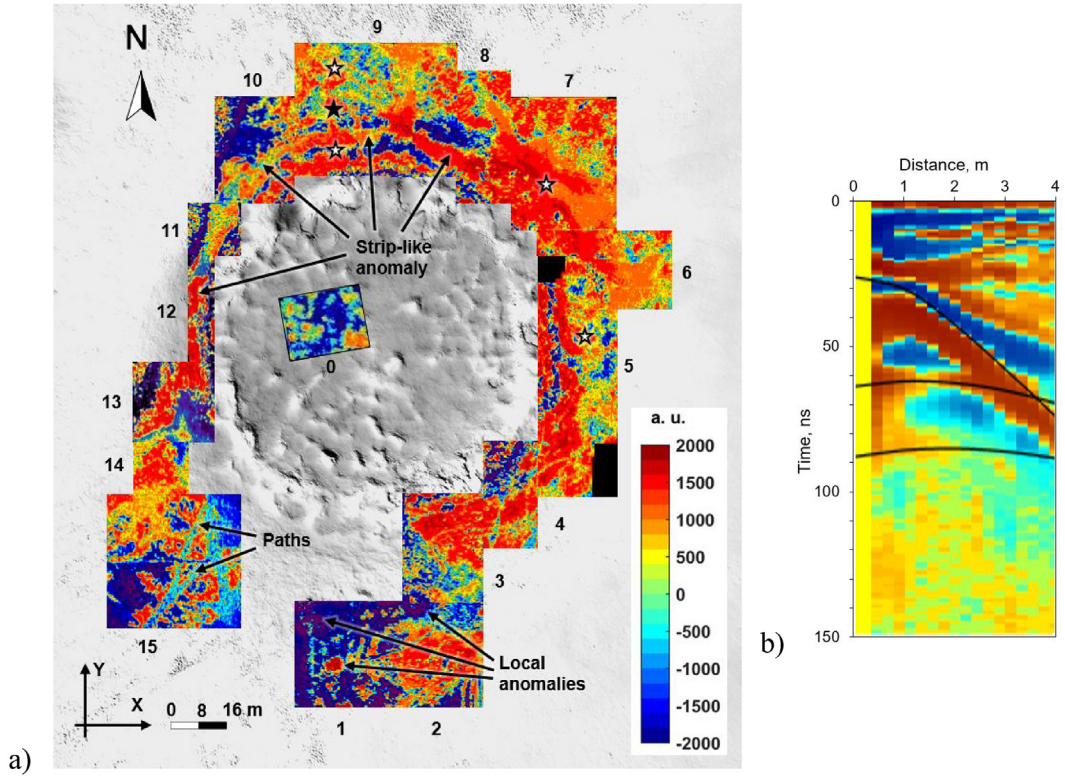

Fig. 3. (a) GPR sounding of the mound periphery. Horizontal section at the 15 ns mark (depth ~ 0.5 m): Nos 0–15 – geophysical sites with the results of GPR sounding. The points of CMP measurements are shown by stars. (b) The CMP hodograph for the point marked with black star in (a) map; black lines correspond to the estimated velocities 0.04, 0.09, 0.084 m/ns (from top down).

Fig. 4. Geological section, excavation. (0) – Modern soil-forming layer (removed) with a stone masonry; (1) – loam; (2) – buried meadow-alluvial soils; (3) – interlayers of sand and loam; (4) – rubble and wood (past river alluvium).

layer that contains a large number of inclusions of crushed stone and gruss (4) (past river alluvium) (El'tsov, 2019; Caspari et al., 2018). The underlying environment of the monument in its natural state is relatively uniform and does not contain enclosing archaeological features, such as stone structures or individual stones.

The radar image of the sub-horizontal structure of the underlying surface is affected by the unevenness of soil moisture saturation, which directly influences the propagation velocity of the electromagnetic waves in the soil. In the upper part of the scan (Fig. 5), the continuous lines of the phase axes have different depths, deeper in zones (1) and (3) compared with zone (2). Changes in the nature of layering of the underlying surface, Fig. 5, occur due to natural uneven thawing depth of the soil, depending on the condition of the grass cover (1), (2) or as a result of human influence – trampling of grass (3) (paths), soil compaction and, as a result, accelerated thawing of the frozen ground. In simple words, the layer depth is more or less constant but the GPR pulse velocity decreases with growing water saturation, so the layers look deeper in the wet zones.

At the time when the measurements were taken, the depth of soil thawing in the periphery of the mound depended on the state of the grass cover, that have been tested by searching stick probes. In the places with thick, dry grass cover, the thawing depth was 0.1–0.15 m. For a thinner cover and on the southern side of the mound, the depth of thawing was 0.2–0.35 m. In the absence of thermo-insulating dry grass cover, the depth of thawing was more than 0.5 m. Maximum soil moisture was observed in the places with a large depth of thawing.

4.2. Feature selection

A GPR mark of artificial objects in a sub-horizontal structure of the underlying surface is given by the following radiophysical features – interruption of the phase axis, waveform peculiarities, numerous phase shifts of the return signal, and presence of multiple reflections. Primary GPR scans (XT plane) allow one to identify the features, determine their sizes, structure and clarify the nature of the anomaly. Horizontal cross-sections allow one to localize objects in the XY plane and purify their characteristic features (dimensions and shape).

In the aerial photograph, Fig. 6a, in the southern part of the mound periphery (site No. 1), a horizontal section of the 3D GPR reconstruction is plotted at the 16 ns time level (depth about 0.5 m). Along with others, two anomalies are clearly seen (indicated by a dotted line). One of them (1) is located at the junction of the site with the excavation and is a continuation of the already discovered stone embankment, while the second one (2), with a diameter of ~8 m, is located in the middle of the site and supposedly presents a constructive base for a burial made of stone.

In the 21 ns XY horizontal section of the 3D model (depth ~ 0.7 m, Fig. 6b) another feature (3) in the middle of the image appears that is more contrasting than the stone embankment and has a pronounced rectangular shape. In another horizontal section of the 3D model, corresponding to the 27 ns mark (depth ~ 1.0 m, Fig. 6c), two features (2,3) are simultaneously observed in the center of the site, close to each other and oriented along the north-south line. On XY GPR sections (Fig. 6b-c), smaller archaeological features along the northern edge of the site were also recorded. According to the schedule of geophysical studies, excavations of the periphery of the mound began only in the second part of the 2019 season, preliminary results, combined with a georadar section of 41 ns (~ 1.6 m), are presented in Fig. 6d.

These horizontal GPR sections at different depths of the patch No. 1 reveal the irregularity of frozen soils thawing. In the eastern part of the site, the depth of thawing is higher than in the rest of the site due to the dense grass cover and amounts to about 0.7 m, which manifests itself in a changed color scale and increasing amplitude of the reflected signal from this boundary.

The use of two geophysical methods (magnetometry and GPR), when examining an archaeological feature, significantly improves the survey quality and increases reliability of the results. For instance, according to the results of the magnetic survey, in the center of the plot No. 1, Fig. 7b, a stone structure (embankment) in the form of an ellipse was found, but, based on magnetometric data alone, it was impossible to judge about the presence of burial under the stone embankment, its

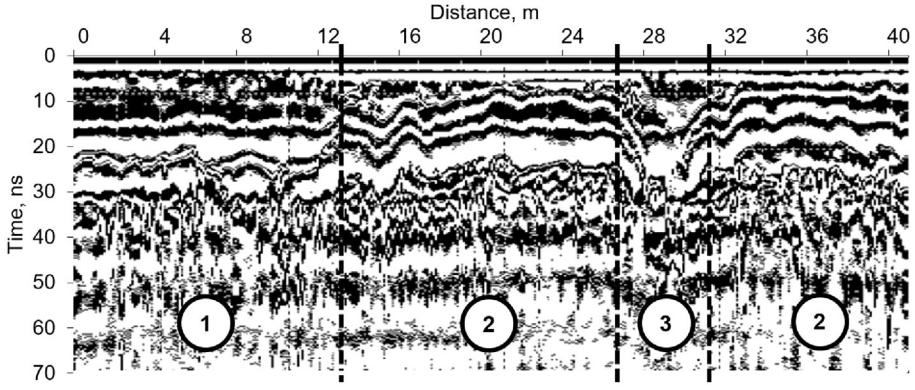

Fig. 5. GPR scan of a sub-horizontal structure of the underlying surface, site No. 15: (1) – regular high humidity zone, thawing depth more than 0.5 m; (2) – zone with regular low humidity structure, small thawing depth; (3) – a feature, thawed high humidity compacted soil.

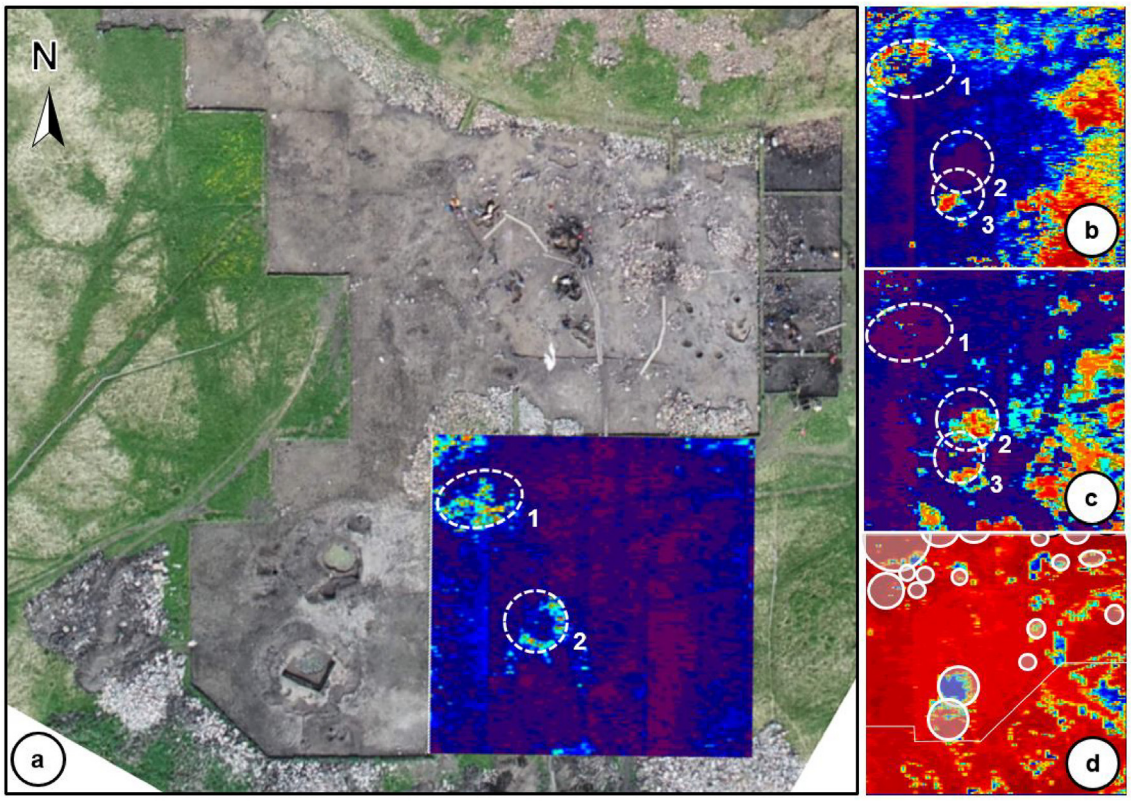

Fig. 6. Site No 1. Aerial view of the mound excavation with horizontal cross-sections of the 3D GPR model: (a) – aerial photograph with a GPR section at 16 ns time level (depth ~ 0.5 m); (b) – 21 ns GPR section (depth ~ 0.7 m); (c) – 27 ns GPR section (depth ~ 1.0 m); (d) – 41 ns GPR section (depth ~ 1.6 m) combined with a map of archaeological sites excavated in 2019. All GPR maps have the same size 32 by 32 m.

size, and depth. On the XY slice of the volumetric GPR map (Fig. 7a), two features correspond to this structure. Feature (2) on the GPR scan (Fig. 7c), bounded by two inclined walls forming a burial pit, and "ringing" of the return signal below indicate the presence of a cavity with unconsolidated soil or two contrast boundaries at a depth of about 1.2–1.4 m (33 ns time level). Artifact (1) is probably located outside the stone embankment since there is no explicit radar image of the stone embankment, the depth of the feature, basing on Fig. 7c, does not exceed 1.0 m (27 ns time level). It can be assumed that the feature (2) refers to an earlier burial than the feature (1).

Magnetometry allows one to localize only those archaeological features, that include structures made of magnetic contrast, in this case, stone structures. The use of GPR can greatly complement the results of magnetometry in the case when the archaeological features are radiocontrast relative to the surrounding medium. On the magnetic map parts in Fig. 2, elongated along the northern and eastern edges of the mound, a stone belt is clearly seen as a discontinuous strip of elongated anomalies placed at a distance of 12–16 m from the shaft surrounding the mound. One of the elements of this design is shown in Fig. 8b, site No. 10. The radargrams (Fig. 3a) reveal interruptions of the regular layering between the shaft and the stone ring of the mound. This feature, 6–8 m wide, enclosed with soil of high humidity (Fig. 8a) has a regular trapezoidal shape (1) on a radargram (Fig. 8c). In its structure, it resembles a ditch or a buried river bed around a mound, in some places up to 1.5 m deep (40 ns time level), and severely destroyed and practically not observed in other parts. The excavated soil

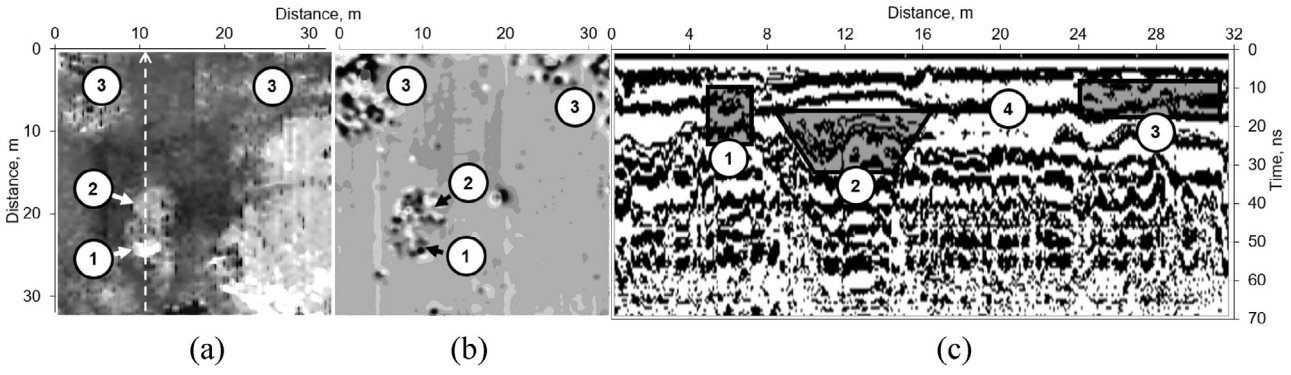

Fig. 7. GPR and magnetometric maps of site No. 1: (a) – horizontal (XY) GPR section at 27 ns time level (depth ~ 1.0 m); b) – magnetic map of the site; c) – GPR profile along the path indicated by a dotted line in (a). Features marked: (1), (2), (3) – archaeological features; (4) – undisturbed sub-horizontal structure.

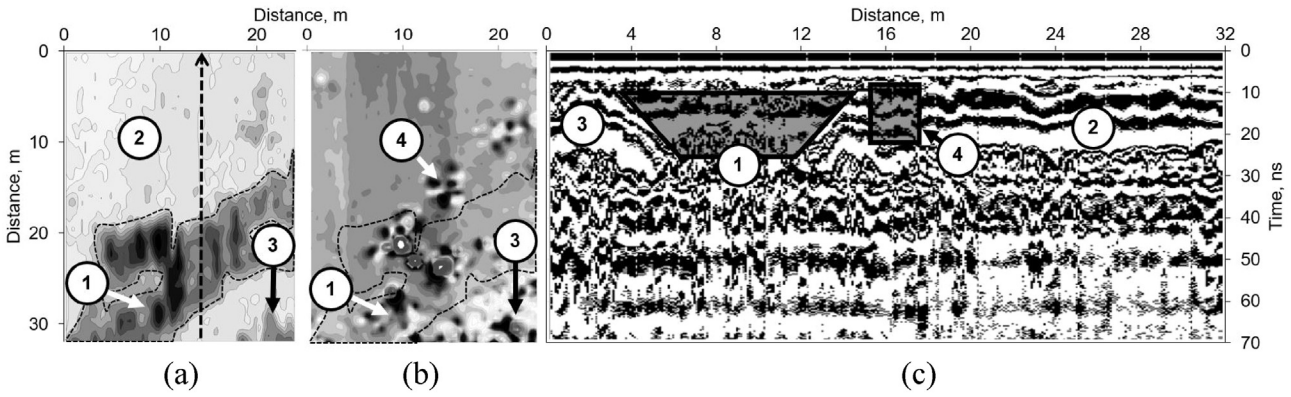

Fig. 8. Survey site No. 10: a) – 3D GPR image of a ditch encircling the mound; b) – magnetic map of the site with a fragment of a stone ring and GPR contour of the moat; c) – GPR scan along the path indicated by a dotted line in (a). Notations: (1) – buried ditch; (2) – undisturbed radiocontrast layers; (3) – a shaft around the mound; (4) – archaeological feature.

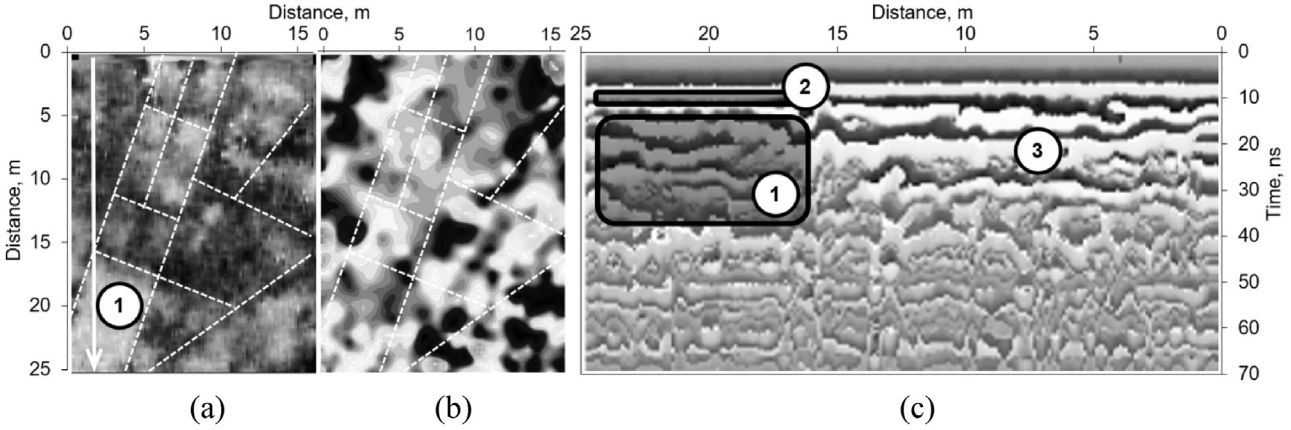

Fig. 9. Site No 0. (inside the mound): a) – horizontal GPR section of a 3D model at 20 ns time level; b) – magnetic map of the site; c) –fragment of the GPR scan along the path indicated by a white solid line in (a). Notations:(1), (2) – archaeological features; (3) – zone with undisturbed underlying ground.

probably was used to create a dump rampart around the mound or to build the mound itself.

A survey was carried out, using magnetometry and GPR, inside the mound. The site was selected in the northwestern part of the mound with a size of 25 by 16 m on a relatively flat area without pits and significant elevations (patch No 0 in Fig. 3a). GPR survey in this area showed the presence of radial architecture of the mound with an irregular structure of burial chambers of rectangular or trapezoidal shapes. In the picture displayed in Fig. 9a, first of all, a rectangular section (1) can be distinguished, characterized by a uniform upper layer (2) – unlike the rest of the spot, the upper layer of which is heterogeneous, presumably due to rock fragments laid during the construction of the mound. This feature extends beyond the selected site towards the center of the mound. According to a GPR profile (Fig. 9c), one can estimate the depth of the base of the human made feature as 1.5–1.7 m (40 ns time level). Near the peg 16 m, a radar image of a V-shaped inhomogeneity is observed, which is characteristic for a vertical wall limiting this feature. On most other GPR scans, interruptions of sub-horizontal equiphase lines also can be observed, which is presumably a result of the works performed during the construction of the mound and may indicate the presence of archaeological features. These are seen in Fig. 9a in the form of dark spots.

On the magnetogram of the spot No 0 (Fig. 9b), an uneven distribution of rock fragments is observed, without the formation of pronounced stone structures. However, the radial orientation of the architecture of the mound is also traced on the magnetogram.

The results of the examining subsurface medium by two geophysical methods – ground penetrating radar and magnetometry have shown the effectiveness of their joint use in studying the periphery of the early Scythian mound. Using magnetometry, it was possible to localize buried stone embankments (ritual walls at the place of burial or sacrifice) and the stone ring around the mound, while, thanks to georadar, it was possible to detect the ditch between the shaft and the stone ring, burial places under stone embankments, as well as to confirm the general tomb architecture, consisting of the radially diverging from the center and forming circular rows.

To conclude, the kurgans of the Kings Valley in Tuva can be considered as an ideal site for integrated geophysical prospecting that shows well-interpretable archaeological results.

5. Conclusion

The use of two geophysical methods operating on different physical principles gives a reliable and entire structure view of such a complex burial place as early Scythian mound Tunnug 1. Ground penetrating radar and magnetometry are mutually reinforcing and increase the chance of success in a geophysical survey of complex archaeological sites even in difficult, poorly drained, swampy areas and in the presence of perennial frozen and unevenly thawing soils as are characteristic for Tuva region.

The method of magnetometry with great accuracy fixed the stone structures of the monument while GPR provided a detailed study of

the design and geometry of burials, the features that are not magnetically contrast. With the help of GPR, the sites of excavation (localization of sub-horizontal structures of the underlying surface) were localized, thereby additional information could be obtained to understand the process of creating the monument.

The use of geophysical methods has led to the discovery of a number of stone structures on the southern periphery of the mound, a well-preserved stone ring in the southern and western parts of the periphery of the mound, a buried moat, possibly a river bed, between a rampart and a stone ring, up to 1.5 m deep.

Declaration of Competing Interest

None.

Acknowledgments

The work was supported by the Russian Foundation for Basic Research, grant No. 18-02-00185 and assisted by the Expedition Center of the Ministry of Defense of the Russian Federation and the Russian Geographical Society.

References

Barone, P.M., Wueste, E., Hodges, R., 2020. Remote sensing materials for a preliminary archaeological evaluation of the Giove Countryside (Terni, Italy). Remote Sens. 12, 2023. https://doi.org/10.3390/rs12122023.

Bevan, B., 2000. An early geophysical survey at Wiliamsburg, USA. Archaeol. Prospect. 7, 51–58. https://doi.org/10.1002/(SICI)1099-0763(200001/03)7:1<51::AID-ARP128>3.0.CO;2-I.

Bianco, C., De Giorgi, L., Giannotta, M.T., Leucci, G., Meo, F., Persico, R., 2019. The Messapic Site of Muro Leccese: New results from integrated geophysical and archaeological surveys. Remote Sens. 11, 1478. https://doi.org/10.3390/rs11121478.

Caspari, G., Sadykov, T., Blochin, J., Hajdas, I., 2018. Tunnug 1 (Arzhan 0) – an early Scythian kurgan in Tuva Republic, Russia. Archaeol. Res. Asia 15, 82–87. https://doi.org/10.1016/j.ara.2017.11.001.

Caspari, G., Sadykov, T., Blochin, J., Buess, M., Nieberle, M., Balz, T., 2019. Integrating remote sensing and geophysics for exploring early nomadic funerary architecture in the "Siberian Valley of the Kings". Sensors 19 (14), 3074. https://doi.org/10.3390/s19143074.

Clark, A., 1990. Seeing beneath the Soil: Prospecting Methods in Archaeology. 1st ed. Routledge, London https://doi.org/10.4324/9780203164983.

Conyers, L.B., 2016. Ground Penetrating Radar for Geoarchaeology. Wiley, Hoboken https://doi.org/10.1002/9781118949993.

Čugunov, K., Parzinger, H., Nagler, A., 2010. Der Skythenzeitliche Fürstenkurgan Aržan 2 in Tuva: Archäologie in Eurasien 26. Steppenvölker Eurasiens 3. Mainz: Philipp von Zabern.

Di Maio, R., Manna, M., Piegari, E., 2016. 3D reconstruction of buried structures from magnetic, electromagnetic and ERT data: example from the archaeological site of phaistos (Crete, Greece). Archaeol. Prospect. 23, 3–13. https://doi.org/10.1002/arp.1516.

Edemsky, D.E., Popov, A.V., Prokopovich, I.V., Sadykov, T.R., Caspari, G., Blochin, J.K., 2020. Magnetic survey of the peripheral areas of the kurgan Tunnug-1 in Tuva. Theory Pract. Archaeol. Res. 29 (1), 100–109. https://doi.org/10.14258/tpai(2020)1(29).-06 (in Russian).

El'tsov, M.V., 2019. Soil and archaeological research of the Tunnug1 mound (Republic of Tuva). Alluvial archaeology: relief, paleoenvironment, occupation history. Proceedings of Seminar, April, 23, 2019, pp. 31–34 https://doi.org/10.31453/kdu.ru.91304.0034.

Fassbinder, J.W.E., 2016. Magnetometry for archaeology. In: Gilbert, A. (Ed.), Encycl. Earth Sci. Series. Springer, Dordrecht, The Netherlands, pp. 499–514 https://doi.org/10.1007/978-1-4020-4409-0_169.

Fassbinder, J.W.E., Becker, H., 2010. Der skythenzeitliche Fürstenkurgan Arzan 2 in Tuva: Die Magnetometerprospektion. Archäologie in Eurasien 26, 19–21.

Fernandez-Alvarez, J.P., Rubio-Melendi, D., Castillo, J.A.Q., Gonzalez-Quiros, A., Cimadevilla-Fuente, D., 2017. Combined GPR and ERT exploratory geophysical survey of the me-dieval Village of Pancorbo Castle (Burgos, Spain). J. Appl. Geophys. 144, 86–93. https://doi.org/10.1016/j.jappgeo.2017.07.002.

Gaffney, C., Gater, J., 2003. Revealing the Buried Past: Geo-Physics for Archaeologists. Tempus Publishing, Stroud https://doi.org/10.1002/arp.275.

Gaidash, S.P., Belov, A.V., Abunina, M.A., Abunin, A.A., 2017. Space weather forecasting at IZMIRAN. Geomagn. Aeron. 57, 869–876. https://doi.org/10.1134/S0016793217070088.

Jol, H.M. (Ed.), 2009. Ground Penetrating Radar: Theory and Applications. Elsevier, Amsterdam https://doi.org/10.1016/B978-0-444-53348-7.X0001-4.

Kopeikin, V.V., Krasheninnikov, I.V., Morozov, P.A., Popov, A.V., Guangyou, Fang, Xiaojun, Liu, Bin, Zhou, 2007. Experimental verification of Loza-V GPR penetration depth and signal quality. Proc. 4th Internat. Workshop on Advanced GPR, Naples, Italy, pp. 230–233 https://doi.org/10.1109/AGPR.2007.386558.

Leucci, G., Masini, N., Rizzo, E., Capozzoli, L., De Martino, G., De Giorgi, L., Marzo, C., Roubis, D., Sogliani, F., 2015. Integrated archaeogeophysical approach for the study of a medieval monastic settlement in Basilicata. Open Archaeol. 1, 236–246. https://doi.org/10.1515/opar-2015-0014.

Linck, R., Kaltak, A., 2019. Drone radar: a new survey approach for Archaeological Prospection? Proc. 13th International Conference on Archaeological Prospection, Sligo, Ireland, pp. 268–271 https://doi.org/10.32028/9781789693072

Maki, D., Fields, R.C., 2010. Multisensor geophysical survey results from the Pine tree Mound Site: a comparison of geophysical and excavation data. Southeast. Archaeol. 29 (2), 292–309. https://doi.org/10.2307/41620243.

Parzinger, H., Gass, A., Fassbinder, J., 2016. The latest geoarchaeological and geophysical studies: at the Foot of Royal Kurgans. Sci. First Hand 1, 74–89.

Prokopovich, I., Edemsky, D., Popov, A., Morozov, P., 2018. GPR survey of fortification objects on Matua island. Proc. 17th Internat. Conference on Ground Penetrating Radar, Rapperswil, Switzerland, pp. 47–50 https://doi.org/10.1109/ICGPR.2018.8441644.

Ruhunusiri, W.D.S., Jayananda, M.K., 2008. Construction of a proton magnetometer. Proc. Tech. Sessions 24, 78–85.

Sadykov, T., Caspari, G., Blochin, J., 2020. Kurgan Tunnug 1 – new data on the earliest horizon of Scythian material culture. J. Field Archaeol. 45 (8), 556–570. https://doi.org/10.1080/00934690.2020.1821152.

Schmidt, A., 2009. Electrical and magnetic methods in archaeologicalprospection. In: Campana, S., Piro, S. (Eds.), Seeing the Unseen Geophysicsand Landscape Archaeology. CRC Press/Balkema, London, UK https://doi.org/10.1201/9780203889558.pt2.

Welc, F., Mieszkowski, R., Vrkljan, G.L., Konestra, A., 2017. An attempt to integration of different geophysical methods (magnetic, gpr and ert); a case study from the late Roman settlement on the Island of Rab in Croatia. Studia Quaternaria 34 (1), 47–59. https://doi.org/10.1515/squa-2017-0004.

Zaitseva, G.I., Chugunov, K.V., Alekseev, A.Yu., Dergachev, V.A., Vasiliev, S.S., Sementsov, A.A., Cook, G., Scott, E.M., van der Plicht, J., Parzinger, H., Nagler, A., Jungner, H., Sonninen, E., Bourova, N.D., 2007. Chronology of key barrows belonging to different stages of the Scythian period in Tuva (Arzhan-1 and Arzhan-2 barrows). Radiocarbon 49 (2), 645–658. https://doi.org/10.1017/S0033822200042545.

Zhao, E., Tian, G., Forte, E., Pipan, M., Wang, Y., Li, X., Shi, Z., Liu, H., 2015. Advances in GPR data acquisition andanalysis for archaeology. Geophys. J. Int. 202, 62–71. https://doi.org/10.1093/gji/ggv121.